Alternative splicing of ANLN synergistically contribute to the progression of head-neck squamous cell carcinoma

Erliang Guo
Second Affiliated Hospital of Harbin Medical University
xionghui Mao
Harbin Medical University Third Hospital: Tumor Hospital of Harbin Medical University
Lunhua Guo
Harbin Medical University Third Clinical College: Tumor Hospital of Harbin Medical University
Changming An
Chinese Academy of Medical Sciences Cancer Institute and Hospital: Cancer Hospital Chinese Academy of Medical Sciences
Cong Zhang
Harbin Medical University Third Clinical College: Tumor Hospital of Harbin Medical University
Kaibin Song
Harbin Medical University Third Hospital: Tumor Hospital of Harbin Medical University
Guohui Wang
Harbin Medical University Third Clinical College: Tumor Hospital of Harbin Medical University
Chunbin Duan
Harbin Medical University Third Clinical College: Tumor Hospital of Harbin Medical University
Xiwei Zhang
Chinese Academy of Medical Sciences Cancer Institute and Hospital: Cancer Hospital Chinese Academy of Medical Sciences
Xianguang Yang
Harbin Medical University Third Hospital: Tumor Hospital of Harbin Medical University
Zhennan Yuan
Harbin Medical University Third Clinical College: Tumor Hospital of Harbin Medical University
Ji Sun
Harbin Medical University Third Clinical College: Tumor Hospital of Harbin Medical University
Xiaomei Li
Harbin Medical University Third Clinical College: Tumor Hospital of Harbin Medical University
Weiwei Yang
Harbin Medical College: Harbin Medical University
Hongxue Meng

Harbin Medical University Third Hospital: Tumor Hospital of Harbin Medical University

Susheng Miao (drmiaosusheng@126.com)

Harbin Medical University Third Hospital: Tumor Hospital of Harbin Medical University

---

Research Article

Keywords: ANLN, alternative splicing, HNSCC, exosomes, macrophage polarization

Posted Date: February 24th, 2021

DOI: https://doi.org/10.21203/rs.3.rs-233563/v1

Abstract

Objective

Head and neck squamous cell carcinoma (HNSCC) is a common cancer with high mortality. Anillin (ANLN) has been identified as an actin-binding protein highly expressed in multiple cancers. However, the expression pattern and functional effects of ANLN in HNSCC remains to be unclear.

Methods

ANLN alternative splicing was assessed in HNSCC tissues and cell lines. We investigated the functional effects and related mechanisms of ANLN alternative splicing in HNSCC *in vitro* and *in vivo*.

Results

Our results showed that two ANLN alternative RNA splicing ANLN-201 and ANLN-210 were highly expressed in HNSCC tissues and cell lines. Knockout of ANLN led to inhibited proliferation, migration and invasion of SCC-9 cells. ANLN-201 mainly binded to Myc and thus played a role in promoting cell proliferation, migration and invasion of SCC-9. ANLN-210 was found to bind mainly to HNRNPC and secreting into the environment in the form of exosomes. Exosomal ANLN-210 promotes macrophage polarization via PTEN/PI3K/Akt signaling pathway, which in turn facilitated HNSCC tumor growth.

Conclusions

Variable alternative splicing of ANLN synergistically contribute to the progression of head-neck squamous cell carcinoma, which might offer new perspectives of HNSCC for treatment strategies.

Introduction

Head and neck squamous cell carcinoma (HNSCC) has been identified as the sixth most common cancer in the world [1,2]. Squamous cell carcinoma (SCC) is the major pathological pattern of head and neck squamous cancer. Although improvements have been made in diagnosis and treatment strategies, patients with HNSCC at advanced stages may develop visceral metastases and present a poor prognosis with low five-year survival rates [3–5]. It is necessary to explore the underlying molecular mechanisms of HNSCC and identify novel effective biomarkers for diagnosis and treatment of HNSCC.

Anillin (ANLN) which is located on chromosome 7p14.2 and encodes an actin-binding protein containing 1125 amino acids, has been identified to play a vital role in actin cytoskeletal dynamics [6–8]. Increasing studies have shown that ANLN is highly expressed in multiple cancers, including breast cancer, ovarian cancer, kidney cancer, colorectal cancer, hepatocellular carcinoma, lung cancer, and pancreatic tumors [9–

[14]. Recent studies indicate that dysregulated ANLN contributes to the tumor occurrence, growth and development. For instance, it was reported that ANLN promoted pancreatic cancer progression by regulating EZH2/miR-218-5p/LASP1 signaling axis [15]. ANLN promoted doxorubicin resistance in breast cancer cells by activating RhoA [16]. ANLN played a critical role in human lung carcinogenesis through the activation of RHOA and by involvement in the phosphoinositide 3-kinase/AKT pathway [17]. Nevertheless, biological functions and regulatory mechanisms of ANLN involved in head-neck squamous cell carcinoma progression are not quite clear.

Alternative RNA splicing in eukaryote which could enables cells to have various transcript isoforms and protein diversity from a single gene, plays pivotal roles during normal biological processes such as tissue and organ development [18,19]. RNA splicing is a highly regulated process and accumulating evidence have shown that splicing is frequently occurred in human tumors. Diverse spliceosomes which enable different biological functions are common in cancers and might together lead to malignant cellular transformation [18,20,21]. Studies have suggest that coordinated splicing networks might regulate tumor development and thus provide novel potential therapeutic targets of human cancer treatment.

It is reported that Pacific Bioscience (PacBio) long-read sequencing has been used to identify full-length transcripts and splicing junctions [22–24]. In our previous study, we analyzed ANLN RNA splicing using PacBio and found that there were two spliceosomal form of ANLN in HNSCC, that was, ANLN-201 (ENST00000265748.7, 4731 nt) and ANLN-210 (ENST00000457743.1, 757 nt).

This study was the first to investigate the expression pattern, diverse functions and regulatory mechanisms of two spliceosomes of ANLN in HNSCC tissues and cell lines. The involved signaling pathways of two ANLN spliceosomes on HNSCC carcinogenesis were also investigated.

Methods And Materials

Tissues samples

Human head and neck tumor tissues and paired adjacent non-tumor tissues were obtained from patients at the Harbin Medical University Cancer Hospital (Harbin, China). Both tumor tissues and non-tumor tissues were evaluated histologically. Written or oral consent was provided by all of the involved patients and the Ethics Committee of Harbin Medical University Cancer Hospital approved all aspects of this research.

Cell lines and cell culture

Human head and neck squamous carcinoma cell lines SCC9, SCC15, FaDu were grown in DMEM/F12 (Invitrogen, Carlsbad, CA, USA) containing 10% fetal bovine serum (FBS, Gibco). Human bronchial epithelial cell line BEAS-2B were cultured in DMEM supplemented with 10% LHC-9 medium (Invitrogen) and 10% FBS (Gibco). Human hepatocellular carcinoma cell line HepG2, human colorectal cancer cell line HCT-116 and Breast cancer cell line MCF-7 were cultured in DMEM supplemented with 10% FBS.

Laryngeal squamous cell carcinoma cell line SNU899 was maintained in RPMI-1640 (Gibco) with 10% FBS (Gibco). Human monocytic THP-1 cells were maintained in RPMI 1640 containing 10 % of heat inactivated FBS and supplemented with 10 mM Hepes (Gibco), 1 mM pyruvate (Gibco), 2.5 g/l D-glucose (Merck) and 50 pM ß-mercaptoethanol (Gibco). THP-1 monocytes were differentiated into macrophages incubated with 150 nM PMA (Sigma) followed for24 h. These cancerous cell lines were maintained in a humidified incubator at 37°C with 5% CO_2.

Quantitative real-time PCR (qRT-PCR)

Total RNA was extracted with TRIzol reagent and reverse transcribed to cDNA using a PrimeScript RT reagent kit (TaKaRa, Tokyo, Japan) according to the manufacturer's instructions. Quantitative real-time PCR (qRT-PCR) was performed using the SYBR Green qPCR Master Mix (Takara). The sequences of primers were listed in Table 1

Table 1
Primers of gene for qRT-PCR

Genes	Sequences
GAPDH	Forward:5'-TGGATTTGGACGCATTGGTC-3'
	Reverse: 5'-TTTGCACTGGTACGTGTTGAT-3'
ANLN-201	Forward: 5'-ATGTCTTCGTGGCCGATTTGA-3'
	Reverse: 5'-CTCTGACAGTGAGTTTCCTGTTT-3'
ANLN-210	Forward: 5'-TGCCAGGCGAGAGAATCTTC-3'
	Reverse: 5'-CGCTTAGCATGAGTCATAGACCT-3'
MYC	Forward:5'-CTTTCCTCCACTCTCCCTGG-3'
	Reverse: 5'-AACCCTCTCCCTTTCTCTGC-3'
HNRNPC	Forward:5'-GGAGATGTACGGGTCAGTAACA-3'
	Reverse: 5'-CCCGAGCAATAGGAGGAGGA-3'
SRSF10	Forward:5'-TGAGGATGTTCGTGATGCTGA-3'
	Reverse: 5'-CCTCCTTTCATAACTTCGGCTT-3'
U2AF2	Forward:5'-ACCCAGGCTATGGCCTTTG-3'
	Reverse: 5'-GAAGCGGCTGGTAGTCGTG-3'

Northern blot

RNA was extracted and heat denatured at 65°C for 15 min. The prepared RNA samples were loaded in the gel in the MOPS running buffer, which was electrophoresed at 5–6 V/cm until the bromophenol blue (the faster-migrating dye) migrated at least 2–3 cm into the gel. The gel was visualized on a UV transilluminator. The 28S rRNA band should be approximately twice as intense as the 18S rRNA band.

Cell cycle analysis

The harvested SCC-9 cells were resuspended with PBS and fixed overnight with 70% ethanol at 4°C, then incubated with PI staining reagent at room temperature for 30 min. The treated cells were analyzed using a FACS Calibur system (BD Biosciences, San Jose, CA, USA).

Western blot

Proteins were extracted from tissues and cells. The protein concentration was determined by the bicinchoninic acid (BCA) Kit (Beyotime, Shanghai, China). Proteins were separated with 10% sodium dodecyl sulfate-polyacrylamide gel electrophoresis (SDS-PAGE) and transferred to the nitrocellulose membrane. After blocking, the membranes were incubated in primary antibodies at 4°C overnight. ANLN-201 and ANLN-210 (1:1000, GeneX health, Beijing), ANLN (1:1000, ab211872, Abcam, Cambridge, MA, USA). Myc (ab32072), F-actin (ab130935), HNRNPC (ab75822), SRSF10 (ab254935), U2AF2 (PA5-30442, Invitrogen), HSP70 (ab2787), CD63 (ab134045), TSG101(ab125011), Calnexin (ab22595), CD206 (ab125028), Arg-1 (ab133543), PTEN (ab267787), Akt (ab8805), p-Akt (ab38449), GAPDH (ab9485), and β-actin (ab8226), GAPDH and β-actin was used as the internal control. Protein bands were visualized by chemiluminescence (ECL, Forevergen, Guangzhou, China). The experiment was conducted for three times.

Immunoprecipitation

To detect ANLN associated with F-actin/Myc, total protein was extracted from SCC-9 cells after treatment. Cell lysates for immunoprecipitation were pre-cleared and incubated with GFP-protein-magnetic beads overnight at 4°C. The beads were washed and boiled with loading buffer, then for immunoblots with GFP (abcam) antibodies.

Isolation of exosomes

Exosomes were isolated from cell culture medium by ultracentrifugation according to the previous reports [25]. The procedures were performed at 4°C. Briefly, cells were removed by centrifugation at 300g. Other debris were removed by centrifugation at 3,000 g. After that, the supernatants were centrifuged at 10,000 g for 30 min to remove shedding vesicles and others. At last, the supernatants were centrifuged at 110,000 g for 70 min. Exosomes were obtained from the pellets and re-suspended in PBS.

Cell proliferation analysis

Cell proliferation of SCC-9 cells was determined using the Cell Counting Kit-8 (CCK-8; Dojindo Laboratories, Kumamoto, Japan) according to the manufacturer's instructions. SCC-9 cells transfected as

experiments designed were plated in 96-well plate. Cell viability was analyzed for 24, 48, 72, 96h. CCK-8 was added and incubated for 3h according to the time points. The absorbance was measured at 450 nm.

Cell migration and invasion assays

Cell migration and invasion assays were performed using transwell insert chambers (BD Biosciences, USA). SCC-9 cells were transfected as experiments designed. The transfected SCC-9 cells in serum-free medium were seeded into the top chamber. The medium containing 20% FBS was added to the lower chambers. After routinely cultured for the appropriate time, cells on the lower membrane surface of the top chamber were fixed with methanol and stained with DAPI. For invasion analysis, the top chambers were coated with the matrigel (BD Biosciences, USA).

Immunofluorescence

SCC-9 cells were fixed and permeabilized, then incubated with GFP Rabbit antibody (ab290, Abcam) for 3 hours at 4°C. After washing three times with PBS, the cells were incubated with Alexa Fluor 488 conjugated Goat Anti-Rabbit IgG (H&L) (ab150077; Abcam) for 1 h at room temperature in the dark place. After washing three times with PBS, cells were treated with DAPI (D9564, Sigma) for 10 min at room temperature. Cells were photographed using the confocal microscope (Olympus FV-1000).

Immunohistochemistry (IHC)

Paraffin-embedded HNSCC tissues were fixed in 4% polyformaldehyde (PFA). IHC staining was performed according to the manufacturer's protocol. The deparaffinized and rehydrated histologic sections were aimmersed in 10 mM citrate buffer for heat-induced antigen retrieval. The slides were stained using antibodies against CD163 (ab182422, Abcam) and Ki67 (ab15580, Abcam).

Animals

Male BALB/c nude mice (6~8 weeks) were raised strictly in the pathogen-free animal house in accordance with feeding standards, which was approved by the Institutional Animal Care and Research Advisory Committee of XX hospital.

Xenograft models

To assess the effects of exosomal ANLN-210–activiated M2 polarized macrophages on HNSCC tumor growth i*n vivo*, 1.5×10^7 SCC-9 cells were mixed in a 4:1 ratio with the macrophages transfected with exosomes with different treatment as experiment designed. Then the cell mixture was co-injected into the flanks of the nude mice. After 3 weeks, the mice were euthanized and the tumors were obtained and fixed in formaldehyde for and IHC staining.

Statistical analysis

All the experiments were repeated at least three times. The data were analyzed using SPSS 20.0 and GraphPad Prism 7. The P value < 0.05 was considered to be significant.

Results

Variable spliceosomal pattern of ANLN exists in head-neck squamous cell carcinoma

The expression of the spliceosome was different between the cancer tissues and the para-cancer tissues. It was found that ANLN had two forms of spliceosomes, ANLN-201 (ENST00000265748.7, 4731 nt) and ANLN-210 (ENST00000457743.1, 757 nt) in head and neck tumor tissues. However, only ANLN-201 was detected in the corresponding adjacent tissues. We validated ANLN expression in the collected head and neck cancer (HNC) tissues using quantitative PCR and Northern blot. Both ANLN-201 and ANLN-210 were highly expressed in HNC tumor tissues compared to the normal tissues (Figure 1A and 1B). We also found that ANLN-210 (757 nt) was not all highly expressed in HNC tissues (Figure 1C). In addition, we detected the splicing forms of ANLN in different tumor cell lines. Interestingly, the results showed that ANLN-210 was detected in almost all of the tested cell lines whereas the ANLN-210 was only detected in the following cell lines, including the hypopharyngeal carcinoma cell line FaDu, the two tongue squamous cell lines SCC-9 and SCC-15, and the laryngeal carcinoma cell line SNU899 (Figure 1D). These results suggest that the expression of the spliceosomal form of ANLN may be more heterogeneous and more common in the head-neck squamous cell carcinoma.

ANLN-201 contributes to the cell malignancy of SCC-9

To investigate the functional role of ANLN in head and neck tumor, we established stable tongue squamous cell line SCC-9 with ANLN knockout by using CRISPR-Cas9 for further study (Figure 2A). We then assessed the effect of ANLN on the cell malignancy of SCC-9. As shown in Figure 2B-2D, knockout of ANLN directly caused SCC-9 cell proliferation inhibition (Figure 2B), triggered G2/M cell cycle arrest (Figure 2C), and suppressed cell migration and invasion capabilities (Figure 2D). Moreover, the rescue experiments were performed in SCC-9 by overexpressing ANLN-201 or ANLN-210 tagged with GFP in the ANLN-knockout SCC-9 cell line. The results showed that only ANLN-201 overexpression could restore the suppressed cell proliferation, cell migration and cell invasion of SCC-9 cells induced by ANLN knockout (Figure 2E-2F). Nevertheless, overexpression of ANLN-210 does not have these same effects. Interestingly, both ANLN-201 and ANLN-210 expression maintained at a high level at mRNA level (Figure 2G). However, the protein level of ANLN-210 was not detected or much lower expressed in SCC-9 compared to ANLN-201 (Figure 2H and 2I). These findings suggest that ANLN-201 could promote SCC-9 proliferation, migration and invasion while ANLN-210 mRNA may not be effectively translated into protein.

Variable expression pattern and functions of ANLN alternative splicing in HNSCC

F-actin is the classical interacting protein of ANLN. We found that compared to ANLN-201, the structure of ANLN-210 missed the domain interacting with F-actin (Figure 3A). The co-immunoprecipitation result also validated that GFP-ANLN-201 could interact with F-actin whereas GFP-ANLN-210 could not (Figure 3B). It was reported that ANLN could interact with myc [26]. The result also confirmed that there was an interaction between GFP-ANLN-201 and myc but not GFP-ANLN-210 (Figure 3C). Next, we transfected SCC-9 cells with ANLN-201 siRNA or ANLN-210 siRNA (Figure 3D). We observed that the expression of Myc at protein level was obviously decreased in ANLN-201 knockdown cells but had no change in ANLN-210 knockdown cells (Figure 3E). Interestingly, neither GFP-ANLN-201 nor GFP-ANLN-210 knockdown had any effect on the mRNA level of Myc (Figure 3F). Next, we found that ANLN-201 knockdown promoted the polyubiquitination of Myc, while ANLN-210 knockdown did not have this effect (Figure 3G). These results suggested that ANLN-201 expression at protein level could affect the protein stability of Myc. In addition, we found that the protein stability of Myc in the ANLN-knockout SCC-9 cells was rapidly down-regulated compared to the control SCC-9 cell line. Overexpression of ANLN-201 could rescue the protein stability of Myc while the ANLN-210 overexpression had no effect (Figure 3H). Taken together, there are two main spliceosome forms of ALAN mRNA in SCC-9 cells, of which only ANLN-201 protein could interact with Myc and thus to regulate the stability of Myc protein.

ANLN-210 mRNA distributes in the cytoplasm of SCC-9

The result indicated that ANLN-201 protein could interact with Myc and positively regulate the protein stability of Myc. To investigate the significance of the high levels of the ANLN-210 mRNA spliceosome, we explored the subcellular localization of the two spliceosomal ANLN mRNA. We found that ANLN-201 mRNA was mainly located around the nucleus while ANLN-210 mRNA was almost distributed in the cytoplasm in the ANLN-knockout SCC-9 cells with ANLN-201 or ANLN-210 overexpression (Figure 4A). What's more, the RNA stability of ANLN-210 mRNA was significantly higher than that of ANLN-201 mRNA with actinomycin D treatment in SCC-9 cells (Figure 4B). Sequence comparison analysis showed that there was extra 54 nucleotides in the sequence that encoded ANLN-210 protein compared with ANLN-201 (Figure 4C). We found that this sequence corresponded to three potential RNA binding proteins sites, including SRSF10, U2AF2 and HNRNPC, analyzed by RBPmap online tool (http://rbpmap.technion.ac.il/) (Figure 4D). Next, we validated that the predicted protein HNRNPC could effectively bind to ANLN-210 mRNA (Figure 4E). These results suggest that ANLN spliceosomes have the different subcellular localization and the corresponding RNA binding protein.

ANLN-210 mRNA interacts with HNRNPC

To further explore the relationship between ANLN-210 mRNA and HNRNPC, we knocked down HNRNPC in SCC-9 cells (Figure 5A). We observed that the relative mRNA level of ANLN-210 was reduced in HNRNPC-knockdown cells, while either SRSF10 or U2AF2 knockdown had no such effect (Figure 5B). In addition, HNRNPC knockdown accelerated instability of ANLN-210 mRNA in SCC-9 cells with actinomycin D treatment compared to SRSF10 or U2AF2 knockdown (Figure 5C). Moreover, we constructed the mutant plasmid that the binding sites between HNRNPC and ANLN-210 were mutated (Figure 5D). As we can see

in Figure 5E, the binding complex between HNRNPC and ANLN-210 RNA could be detected whereas the complex disappeared after transfected with mutant ANLN-210 at the binding sites with HNRNPC. These results indicate that RNA binding protein HNRNPC could interact with ANLN-210 mRNA and maintain the stability of ANLN-210 mRNA.

Interestingly, we found that ANLN-210 expression was increased at protein level with GFP-ANLN-210 transfection with HNRNPC knockdown in ANLN-knockout SCC-9 (Figure S1A and Figure S1B). These results suggest that HNRNPC also inhibits ANLN-210 protein translation as well as maintains its stability. HNRNPC was also highly expressed in head and neck cancer tissues and cell lines (Figure S1C-S1E). Neither ANLN-201 knockdown nor ANLN-210 knockdown in SCC-9 cells had any effect on the expression of HNRNPC at mRNA and protein levels (Figure S1F and S1G). However, ANLN-210 knockdown reduced HNRNPC subcellular localization in the cytoplasm, more concentrated in the nucleus (Figure S1H). The immunofluorescence results further confirmed that HNRNPC was all located in the nucleus and cytoplasm in wild-type SCC-9 cells; while HNRNPC was basically condensed in the nucleus in ANLN-knockout cells. Overexpression of ANLN-210 could restore the cytoplasmic distribution of HNRNPC but not ANLN-201 overexpression (Figure S1I). The above results indicate that HNRNPC affects ANLN-210 mRNA stability, while ANLN-210 in turn affects the cellular localization of HNRNPC.

Exosomal ANLN-210 promotes M2 polarization of macrophages

It was reported that the ANLN 210 mRNA presented in exosomes of colon cancer cells [27] . We also examined the existence of ANLN-210 mRNA and ANLN-201 mRNA in SCC-9 cells secreted exosomes, and the expression of ANLN-210 mRNA was much higher than that of ANLN-201 mRNA (Figure 6A). When HNRNPC was silenced in SCC-9 cells, the content of ANLN-201 mRNA had no changes while ANLN-210 mRNA in exosomes was dramatically reduced (Figure 6B and 6C). Considering that HNRNPC directly affected the stability of ANLN-210 mRNA and causes the reduced ANLN-210 protein level, we overexpressed ANLN-210 while knocking down HNRNPC in SCC-9 cells. The results showed that although the content of ANLN-210 mRNA in cells foldly increased, but not caused an equal increase in ANLN-210 RNA in exosomes (Figure 6B and 6C). These results suggest that HNRNPC could not only maintain the stability of ANLN-210 mRNA, but also promote the release of ANLN-210 mRNA in exosomal forms. Then we prepared ANLN-210 mRNA enriched in exosomes in two ways. One is to transfect the ANLN-210 plasmid into SSC-9 cells. The other way is to electroporate ANLN-210 mRNA into SSC-9-derived exosomes (Figure 6D-6E). ANLN-210 mRNA levels were much higher in electroporated exosomes compared to the overexpression group (Figure 6F). However, these prepared exosomes rich in ANLN-210 mRNA neither promoted SCC-9 cell proliferation and migration after co-incubation with SCC-9 cells nor promoted hepatocarcinoma cells HepG-2 malignant features (Figure 6G and 6H). Next, it is interesting to investigate the aim of SCC-9 cells to keep high levels of ANLN-210 mRNA in exosomes.

Macrophages existing around tumors, are the most abundant infiltrating immune-related stromal cells. Previous studies have shown that tumor cells released exosomes accelerated tumor growth by promoting tumor-associated macrophages into "M2" type. To explore the functional effects of exosomal ANLN-210

mRNA on macrophages, we induced human leukemia mononuclear cells THP-1 to macrophages with PMA treatment, from suspension to wall attachment (Figure 7A). The expression level of CD68, a macrophage marker was significantly increased (Figure 7B). These results proved that the monocyte THP-1 was successfully differentiate into macrophages, “M0” macrophages. We found that the mRNA levels of M2 markers Arg-1, CD206, IL10 and TGF-β were significantly up-regulated when incubated with the electroporated exosomes with ANLN-210 mRNA or exosomes with ANLN-210 mRNA overexpression compared to control group, while the relative expression of M1 markers iNOS and IL6 had no significant difference, suggesting that exosomal ANLN-210 mRNA could promote macrophage M2 polarization (Figure 7C). If THP-1 cells were co-transfected with locked nucleic acid of anti-ANLN-210 mRNA, the M2 polarization effects caused by exosomal ANLN-210 mRNA could be effectively suppressed (Figure 7D).

It has been recently recognized that PI3K-Akt is one of the most important signaling pathways involved in regulating the polarization of macrophages, and PTEN is a negative regulator of the PI3K pathway. After PMA-induced THP-1 was incubated with ANLN-210-rich exosomes, we observed that PTEN expression was downregulated and p-Akt expression was up-regulation. The locked nucleic acid targeting ANLN-210 RNA could effectively prevent the activation of Akt. (Figure 7D). Next, we examined the effects of M2 macrophages induced by ANLN-210-rich exosomes on the proliferation, migration and invasion of SCC-9 cells. The results showed that, M2 macrophages induced by ANLN-210-rich exosomes could significantly promote SCC-9 cells proliferation compared with the control exosomes derived from the ANLN-knockout cell line (Figure 7E), which has the similar effects on cell migration and invasion (Figure 7F). The above results reveal that ANLN-210 mRNA released in the form of exosomes secreted from SCC-9 may activate macrophages through PTEN/PI3K/Akt signaling pathway, leading to M2 polarization thus promotes SCC-9 cell proliferation, migration and invasion in a feedback manner.

Two ANLN mRNA splicing synergistically promote tumor progression *in vivo*

To further evaluate the role of the two spliceosomes of ANLN in tumor development, we co-injected SCC-9 cells and macrophages treated with ANLN-210 mRNA-rich exosomes into the nude mice. As shown in Figure 8A, the tumor volumn of mice xenografts was increased significantly. Among them, , the tumor volume in the group that SCC-9 cells overexpressing ANLN-201 mRNA mixed with THP-1 cells treated with ANLN-210 mRNA-rich exosomes was the most significantly increased (Figure 8A). Consistently, Ki67-positive cells with Ki67-positive and CD163-positive were the most in the group that SCC-9 cells overexpressing ANLN-201 mRNA mixed with THP-1 cells treated with ANLN-210 mRNA-rich exosomes (Figure 8B). Taken together, the results reveal that the two spliceosomes of ANLN synergistically promote tumor progression in vivo via different mechanisms.

Discussion

ANLN is expressed ubiquitously in human tissues and overexpressed in multiple human tumors. However, the expression pattern and molecular mechanism of ANLN in HNSCC remain unclear. In the present study, we found that ANLN at mRNA level was highly expressed in HNSCC tissues and SCC-9 cells with two

variable alternative splicing forms (ANLN-201 and ANLN-210). Next, we discovered that loss of ANLN inhibited cell proliferation, migration and invasion of SCC-9 cells. Furthermore, we revealed a novel mechanism of these two ANLN RNA splicing cooperatively regulating tumorigenesis of HNSCC in two ways. That is, on one hand, Myc was identified to directly interact with ANLN-201 and keep its protein stability, thus affected cell proliferation, migration, and invasion of SCC-9 cells. On the other hand, HNRNPC was found to be an RNA binding protein of ANLN-210 and keep RNA stability of ANLN-210. SCC-9 cells secreted overexpressed ANLN-210 mRNA delivered to tumor associated macrophages (TAMs) via exosomes, causing activation of macrophages polarized to M2 phenotype via the canonical PI3K/Akt signaling pathway, thus promoting tumor growth and metastasis of HNSCC. These combined regulation of two different alternative splicing of ANLN highlighted the biological functions and regulatory mechanism of ANLN in HNSCC tumorigenesis, which might provide new perspective for cancer therapy.

HNRNPC is one of the family members of ubiquitously expressed heterogeneous nuclear ribonucleoproteins (hnRNPs), which located in the nucleus and plays critical roles in posttranscriptional regulation including roles in alternative splicing, stability and translation [28–30]. It was previously reported that hnRNPC regulated cancer-specific alternative cleavage and polyadenylation (APA) profiles in colon cancer, which has a critical role in cancer progression [31]. In this study, HNRNPC was predicted to be one of the RNA binding proteins of ANLN-210. Next, the interaction between ANLN-210 and HNRNPC was confirmed by RNA-IP. What's more, we found that HNRNPC could maintain ANLN-210 RNA stability as well as prevent its protein translation. In turn, ANLN-210 knockdown promoted HNRNPC accumulation in the nucleus. However, whether HNRNPC is a critical novel regulator of cancer specific APA for ANLN-210 in HNSCC remains to be explored.

It is known that tumor growth and progression is strongly associated with tumor microenvironment, of which solid tumors infiltrate around immune cells. Macrophages, called tumor-associated macrophages (TAMs) are rich in tumor tissues. Multiple studies have shown that macrophages can affect various aspects of tumor development. M2-macrophages play a pivotal role in promoting tumor growth, metastasis, and angiogenesis [32,33]. Previous studies reported that tumor-associated macrophages of the M2 phenotype contributed to progression in gastric cancer with peritoneal dissemination [34]. In bladder cancer, tumor-infiltrating M2 macrophages driven by specific genomic alterations were associated with prognosis [35]. In ovarian cancer cells, miR-21 modulated the polarization of macrophages and increased the effects of M2 macrophages on promoting the chemoresistance of ovarian cancer [36]. In this study, we observed that ANLN-210 overexpression by exosomes activated macrophage to the M2 phenotype as marked by the increased expression of M2 markers Arg-1, CD206, IL-10 and TGF-β. PI3K/Akt signaling pathway has been widely recognized in multiple cell types and functions and emerged as canonical and central regulators of macrophages activation [37]. In this study, we found that exosomal ANLN-210 overexpression regulated M2 polarization by inhibiting the common target PTEN via activating the PI3K/Akt signals.

Tumor-derived exosomes, which are found in all body fluids deliver molecular and genetic messages from tumor cells to normal or other abnormal cells around. Tumor-derived exosomes play key roles in the oncogenic transformation, which have biological and clinical significance for cancer development, cancer progression and even cancer therapy [38]. The attributes of tumor-derived exosomes might be packaged proteins, lipids, or nucleic acids, which could be regarded as biomarkers for cancer diagnosis, prognosis and monitoring treatment responses [39,40]. In 2008, a study reported that there were 4700 distinct mRNAs selectively packaged in exosomes derived from glioblastoma samples [41,42]. It is well known that mRNAs carried by exosomes are involved in critical cellular activities such as cell proliferation, migration, invasion, metastasis, EMT and so on. The present study demonstrates that exosomal ANLN-210 mRNA secreted by SCC-9 promotes macrophages polarization by targeting PTEN via PI3K/Akt. Furthermore, M2 macrophages promoted tumor growth and metastasis of HNSCC. However, it remains to be investigated whether ANLN-210 induces the activation of the PI3K/Akt pathway in the form of RNA or protein.

In summary, our findings demonstrated that the coordinate regulatory networks of ANLN RNA alternative splicing in HNSCC tumor growth and development, which might highlight the perspective for therapeutic strategies of HNSCC.

Conclusions

To sum up, there are two major isoforms of ANLN alternative RNA splicing, ANLN-201 and ANLN-210. ANLN-201 mainly binds to Myc and exists in the nucleus in the form of protein, which can be effectively prevented from degradation and thus play a role in promoting HNSCC cell proliferation, migration, and invasion. ANLN-210 is found to bind mainly to HNRNPC, thus maintains its RNA stability and secreting into the environment in the form of exosomes. Exosomal ANLN-210 promotes macrophage polarization via PTEN/PI3K/Akt signaling pathway, which in turn facilitates HNSCC tumor growth (Fig. 8C). Thus, the variable splicing of ANLN collaboratively regulates HNSCC tumorigenesis in two ways.

Declarations

Ethics approval and consent to participate

Not applicable.

Consent for publication

Yes.

Availability of data and materials

Not applicable

Competing interests

The authors declare that they have no competing interests.

Funding

This work was supported by the National Nature Science Foundation of China (82072985), Postdoctoral Scientific Research Developmental Fund of Heilongjiang Province (LBH-Q18088LBH-Q18076), the N10 Found project of Harbin Medical University Cancer Hospital (2017-03), the Youth Elite Training Foundation of Harbin Medical University Cancer Hospital (JY2016-06), and the Outstanding Youth Foundation of Harbin Medical University Cancer Hospital (JCQN-2018-05) , National Nature Science Foundation of Heilongjiang Province (YQ2020H036), Special funds of central finance to support the development of local University (2019, 2020), Wu-Jieping Medical Foundation (320.6750.19089-22, 320.6750.19089-48).

Authors' contributions

H.M. and S. M. conceived and planned the experiments. L.G., C. A., C. Z., K. S., G. W., C. D., X. Z., X.Y., Z. Y., J.S., X. L. and W. Y performed the experiments. E.G., X.M. wrote the paper. All authors read and edited the manuscript.

Acknowledgements

Not applicable

References

1. Leemans CR, Braakhuis BJ, Brakenhoff RH. The molecular biology of head and neck cancer. Nat Rev Cancer. 2011;11:9–22.
2. Guo T, Califano JA. Molecular biology and immunology of head and neck cancer. Surg Oncol Clin N Am. 2015;24:397–407.
3. Resteghini C, Trama A, Borgonovi E, Hosni H, Corrao G, Orlandi E, et al. Big Data in Head and Neck Cancer. Curr Treat Options Oncol. 2018;19:62.
4. Alsahafi E, Begg K, Amelio I, Raulf N, Lucarelli P, Sauter T, et al. Clinical update on head and neck cancer: molecular biology and ongoing challenges. Cell Death Dis. 2019;10:540.
5. Puram SV, Rocco JW. Molecular Aspects of Head and Neck Cancer Therapy. Hematol Oncol Clin North Am. 2015;29:971–92.
6. Piekny AJ, Maddox AS. The myriad roles of Anillin during cytokinesis. Semin Cell Dev Biol. 2010;21:881–91.
7. Tuan NM, Lee CH. Role of Anillin in Tumour: From a Prognostic Biomarker to a Novel Target. Cancers (Basel). 2020; 12.
8. Piekny AJ, Glotzer M. Anillin is a scaffold protein that links RhoA, actin, and myosin during cytokinesis. Curr Biol. 2008;18:30–6.

9. Wu S, Nitschke K, Heinkele J, Weis CA, Worst TS, Eckstein M, et al. ANLN and TLE2 in Muscle Invasive Bladder Cancer: A Functional and Clinical Evaluation Based on In Silico and In Vitro Data. Cancers (Basel). 2019; 11.
10. Xu J, Zheng H, Yuan S, Zhou B, Zhao W, Pan Y, et al. Overexpression of ANLN in lung adenocarcinoma is associated with metastasis. Thorac Cancer. 2019;10:1702–9.
11. Dai X, Chen X, Hakizimana O, Mei Y. Genetic interactions between ANLN and KDR are prognostic for breast cancer survival. Oncol Rep. 2019;42:2255–66.
12. Wang Z, Chen J, Zhong MZ, Huang J, Hu YP, Feng DY, et al. Overexpression of ANLN contributed to poor prognosis of anthracycline-based chemotherapy in breast cancer patients. Cancer Chemother Pharmacol. 2017;79:535–43.
13. Wang G, Shen W, Cui L, Chen W, Hu X, Fu J. Overexpression of Anillin (ANLN) is correlated with colorectal cancer progression and poor prognosis. Cancer Biomark. 2016;16:459–65.
14. Hall PA, Todd CB, Hyland PL, McDade SS, Grabsch H, Dattani M, et al. The septin-binding protein anillin is overexpressed in diverse human tumors. Clin Cancer Res. 2005;11:6780–6.
15. Wang A, Dai H, Gong Y, Zhang C, Shu J, Luo Y, et al. ANLN-induced EZH2 upregulation promotes pancreatic cancer progression by mediating miR-218-5p/LASP1 signaling axis. J Exp Clin Cancer Res. 2019;38:347.
16. Wang F, Xiang Z, Huang T, Zhang M, Zhou WB. ANLN Directly Interacts with RhoA to Promote Doxorubicin Resistance in Breast Cancer Cells. Cancer Manag Res. 2020;12:9725–34.
17. Suzuki C, Daigo Y, Ishikawa N, Kato T, Hayama S, Ito T, et al. ANLN plays a critical role in human lung carcinogenesis through the activation of RHOA and by involvement in the phosphoinositide 3-kinase/AKT pathway. Cancer Res. 2005;65:11314–25.
18. Urbanski LM, Leclair N, Anczuków O. Alternative-splicing defects in cancer: Splicing regulators and their downstream targets, guiding the way to novel cancer therapeutics. Wiley Interdiscip Rev RNA. 2018;9:e1476.
19. Baralle D, Buratti E. RNA splicing in human disease and in the clinic. Clin Sci (Lond). 2017;131:355–68.
20. Coltri PP, MGP DS, GHG dS. Splicing and cancer: Challenges and opportunities. Wiley Interdiscip Rev RNA. 2019;10:e1527.
21. Montes M, Sanford BL, Comiskey DF, Chandler DS. RNA Splicing and Disease: Animal Models to Therapies. Trends Genet. 2019;35:68–87.
22. Zhang G, Sun M, Wang J, Lei M, Li C, Zhao D, et al. PacBio full-length cDNA sequencing integrated with RNA-seq reads drastically improves the discovery of splicing transcripts in rice. Plant J. 2019;97:296–305.
23. Feng S, Xu M, Liu F, Cui C, Zhou B. Reconstruction of the full-length transcriptome atlas using PacBio Iso-Seq provides insight into the alternative splicing in Gossypium australe. BMC Plant Biol. 2019;19:365.

24. Križanovic K, Echchiki A, Roux J, Šikic M. Evaluation of tools for long read RNA-seq splice-aware alignment. Bioinformatics. 2018;34:748–54.
25. Valadi H, Ekström K, Bossios A, Sjöstrand M, Lee JJ, Lötvall JO. Exosome-mediated transfer of mRNAs and microRNAs is a novel mechanism of genetic exchange between cells. Nat Cell Biol. 2007;9:654–9.
26. Zhang S, Nguyen LH, Zhou K, Tu HC, Sehgal A, Nassour I, et al. Knockdown of Anillin Actin Binding Protein Blocks Cytokinesis in Hepatocytes and Reduces Liver Tumor Development in Mice Without Affecting Regeneration. Gastroenterology. 2018;154:1421–34.
27. Barbagallo C, Brex D, Caponnetto A, Cirnigliaro M, Scalia M, Magnano A, et al. LncRNA UCA1, Upregulated in CRC Biopsies and Downregulated in Serum Exosomes, Controls mRNA Expression by RNA-RNA Interactions. Mol Ther Nucleic Acids. 2018;12:229–41.
28. Wen J, Toomer KH, Chen Z, Cai X. Genome-wide analysis of alternative transcripts in human breast cancer. Breast Cancer Res Treat. 2015;151:295–307.
29. Tremblay MP, Armero VE, Allaire A, Boudreault S, Martenon-Brodeur C, Durand M, et al. Global profiling of alternative RNA splicing events provides insights into molecular differences between various types of hepatocellular carcinoma. BMC Genom. 2016;17:683.
30. Shen Y, Liu S, Fan J, Jin Y, Tian B, Zheng X, et al. Nuclear retention of the lncRNA SNHG1 by doxorubicin attenuates hnRNPC-p53 protein interactions. EMBO Rep. 2017;18:536–48.
31. Fischl H, Neve J, Wang Z, Patel R, Louey A, Tian B, et al. hnRNPC regulates cancer-specific alternative cleavage and polyadenylation profiles. Nucleic Acids Res. 2019;47:7580–91.
32. Sawa-Wejksza K, Kandefer-Szerszeń M. Tumor-Associated Macrophages as Target for Antitumor Therapy. Arch Immunol Ther Exp (Warsz). 2018;66:97–111.
33. Kim J, Bae JS. Tumor-Associated Macrophages and Neutrophils in Tumor Microenvironment. Mediators Inflamm. 2016; 2016: 6058147.
34. Yamaguchi T, Fushida S, Yamamoto Y, Tsukada T, Kinoshita J, Oyama K, et al. Tumor-associated macrophages of the M2 phenotype contribute to progression in gastric cancer with peritoneal dissemination. Gastric Cancer. 2016;19:1052–65.
35. Xue Y, Tong L, LiuAnwei LF, Liu A, Zeng S, Xiong Q, et al. Tumor–infiltrating M2 macrophages driven by specific genomic alterations are associated with prognosis in bladder cancer. Oncol Rep. 2019;42:581–94.
36. An Y, Yang Q. MiR-21 modulates the polarization of macrophages and increases the effects of M2 macrophages on promoting the chemoresistance of ovarian cancer. Life Sci. 2020;242:117162.
37. Vergadi E, Ieronymaki E, Lyroni K, Vaporidi K, Tsatsanis C. Akt Signaling Pathway in Macrophage Activation and M1/M2 Polarization. J Immunol. 2017;198:1006–14.
38. Whiteside TL. Tumor-Derived Exosomes and Their Role in Cancer Progression. Adv Clin Chem. 2016;74:103–41.
39. Zhang X, CYJBXLWGZY Z. The function of tumor-derived exosomes. J BUON. 2019;24:897–904.

40. Shao C, Yang F, Miao S, Liu W, Wang C, Shu Y, et al. Role of hypoxia-induced exosomes in tumor biology. Mol Cancer. 2018;17:120.
41. Skog J, Würdinger T, van Rijn S, Meijer DH, Gainche L, Sena-Esteves M, et al. Glioblastoma microvesicles transport RNA and proteins that promote tumour growth and provide diagnostic biomarkers. Nat Cell Biol. 2008;10:1470–6.
42. Wang Z, Chen JQ, Liu JL, Tian L. Exosomes in tumor microenvironment: novel transporters and biomarkers. J Transl Med. 2016;14:297.

Figures

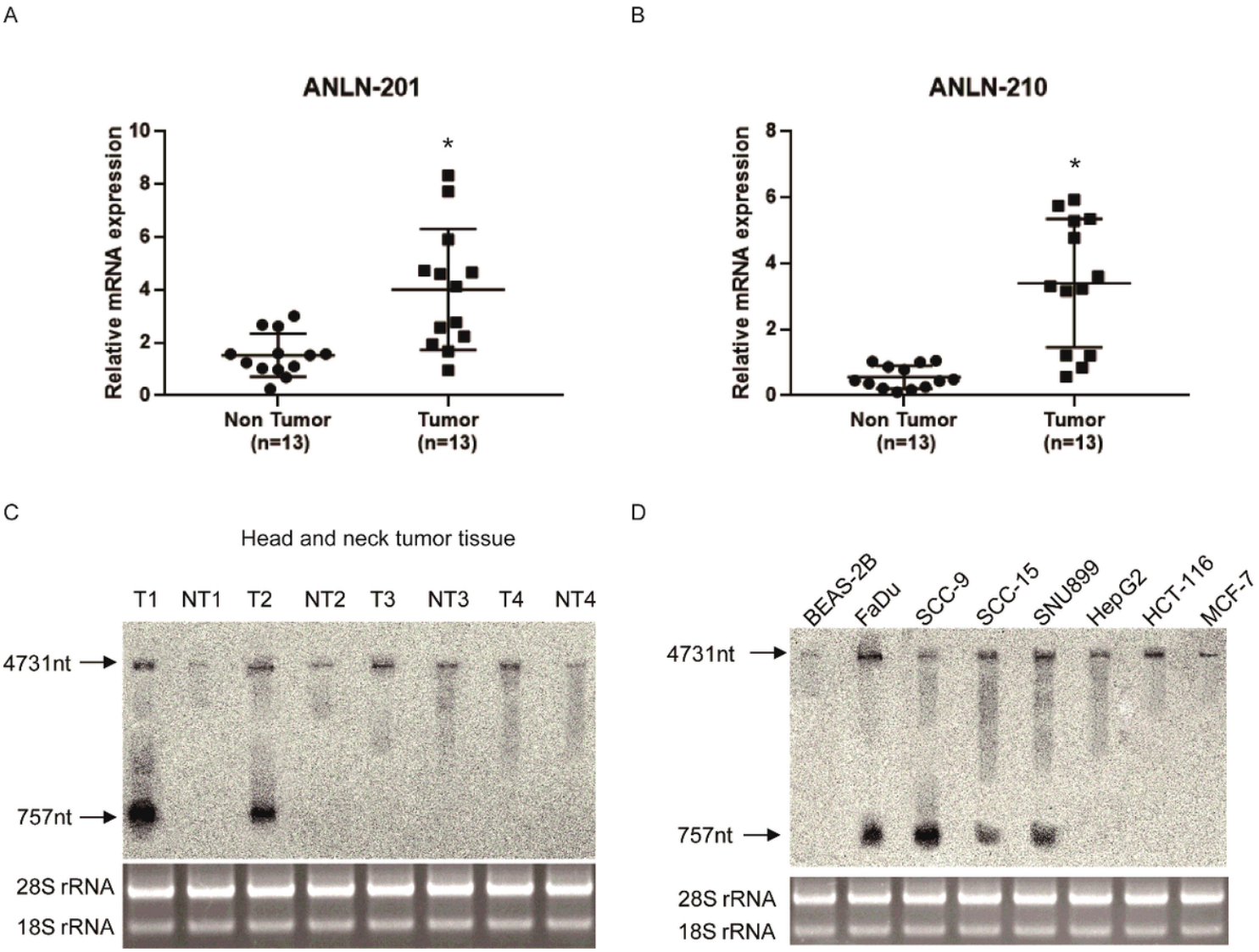

Figure 1

Differential expression of two spliceosomes of ANLN in head-neck squamous cell carcinoma (A and B) The mRNA levels of ANLN-201 and ANLN-210 in head and neck tumor tissues (C and D) Northern blot

analysis using the labeled ANLN-201 or ANLN-210 probe against RNAs from head and neck tumor tissues and several human cancer cell lines.

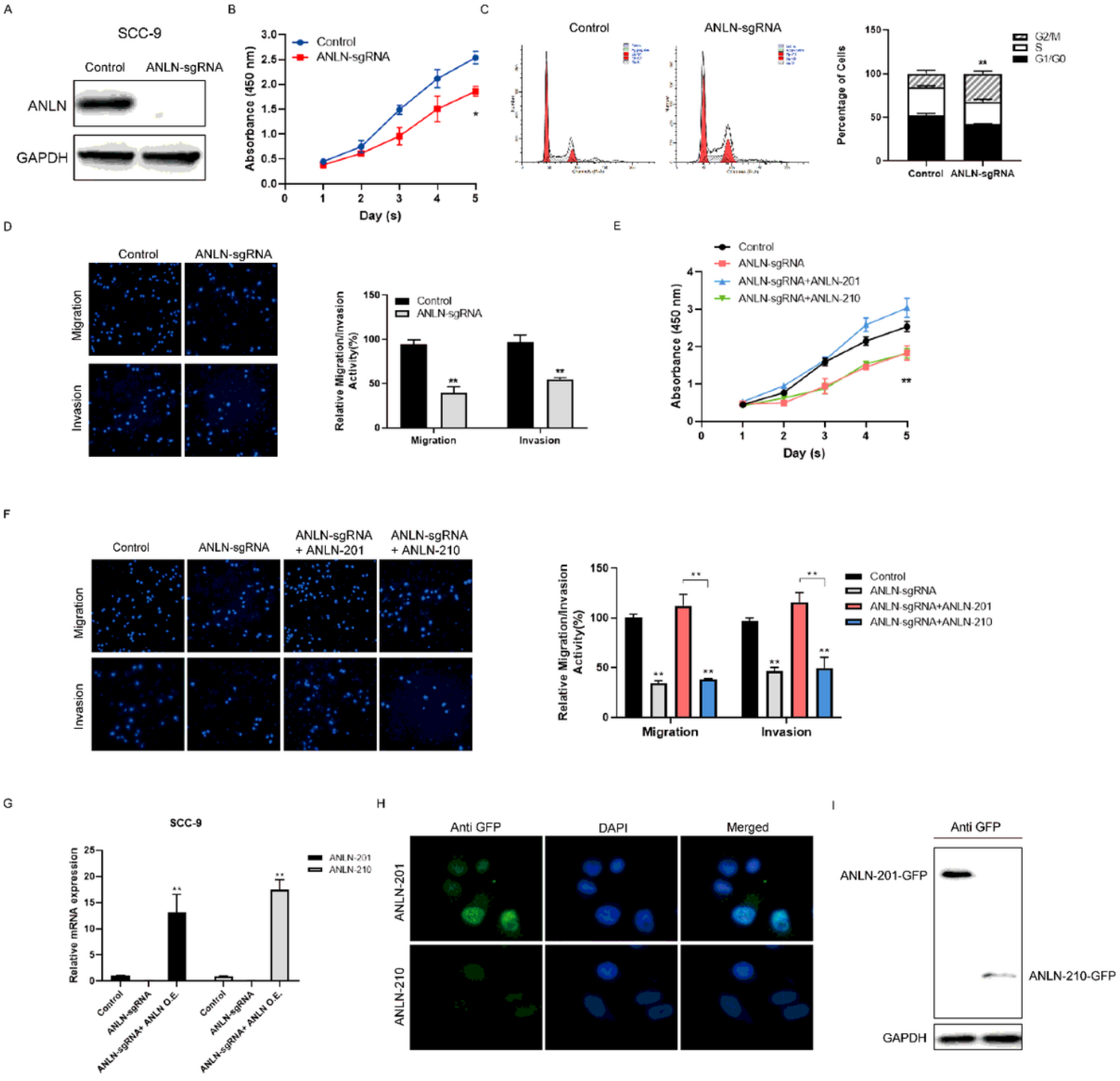

Figure 2

ANLN-201 promotes SCC-9 cell proliferation, migration and invasion (A) ANLN was knocked out in SCC-9 cells using CRISPR/Cas9. (B) Cell counting kit-8 was perform to measure cell proliferation in ANLN-knockout SCC-9 cells.* p□0.05. (C) cell cycle analysis was used to analyze the change of cell cycles induced by ANLN knockout. *p□0.05, **p□0.01. (D) Transwell and transwell-matrigel assay were performed to measure cell migration and cell invasion caused by ANLN knockout. *p□0.05, **p□0.01. (E) Cell

proliferation was assessed in ANLN-knockout SCC-9 cells transfected with ANLN-201 or ANLN-210. *p 0.05, **p0.01. (F) Cell migration and cell invasion were analyzed in ANLN-knockout SCC-9 cells transfected with ANLN-201 or ANLN-210. *p0.05, **p0.01. (G) qRT-PCR was used to examine the m RNA level of ANLN-201 or ANLN-210 in ANLN-knockout SCC-9 cells transfected with ANLN-overexpression plasmid. *p0.05, **p0.01. (H) The immunofluorescence of ANLN-201 and ANLN-210 was assessed in SCC-9 cells using antibody against GFP. (I) ANLN overexpression in SCC-9 cells transfected with recombinant GFP-ANLN-201 or recombinant GFP-ANLN-210. The protein level of ANLN-201 and ANLN-201 was immunoblotted by the antibody against GFP.

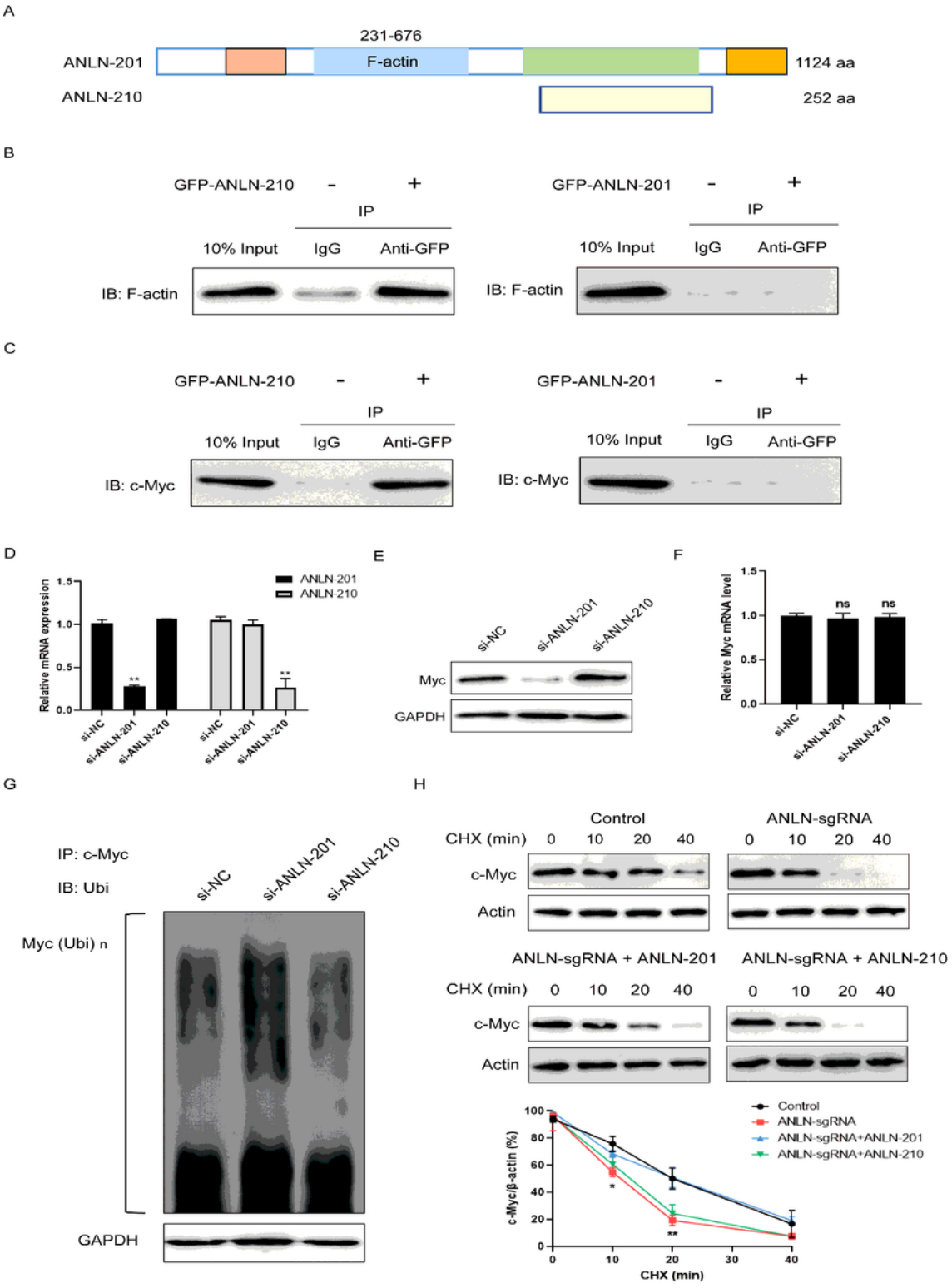

Figure 3

ANLN-210 binds to F-actin while ANLN-201 interacts with Myc. The sequence diagram of ANLN-201 and ANLN-210 was displayed. (B) SCC-9 cells were transfected with recombinant GFP-ANLN-201 or recombinant GFP-ANLN-210. Co-immunoprecipitation was performed between GFP-ANLN-210 or GFP-ANLN-201 and endogenous F-actin in SCC-9 cells. (C) Co-immunoprecipitation was performed between GFP-ANLN-210 or GFP-ANLN-201 and endogenous Myc in SCC-9 cells. (D) The relative mRNA level of

ANLN-201 or ANLN-210 was measured in SCC-9 cells transfected with si-ANLN-201 or si-ANLN-210. (E) The protein level of Myc was examined in ANLN-201 or ANLN-210 knockdown SCC-9 cells. (F) The mRNA level of Myc was examined in ANLN-201 or ANLN-210 knockdown SCC-9 cells.

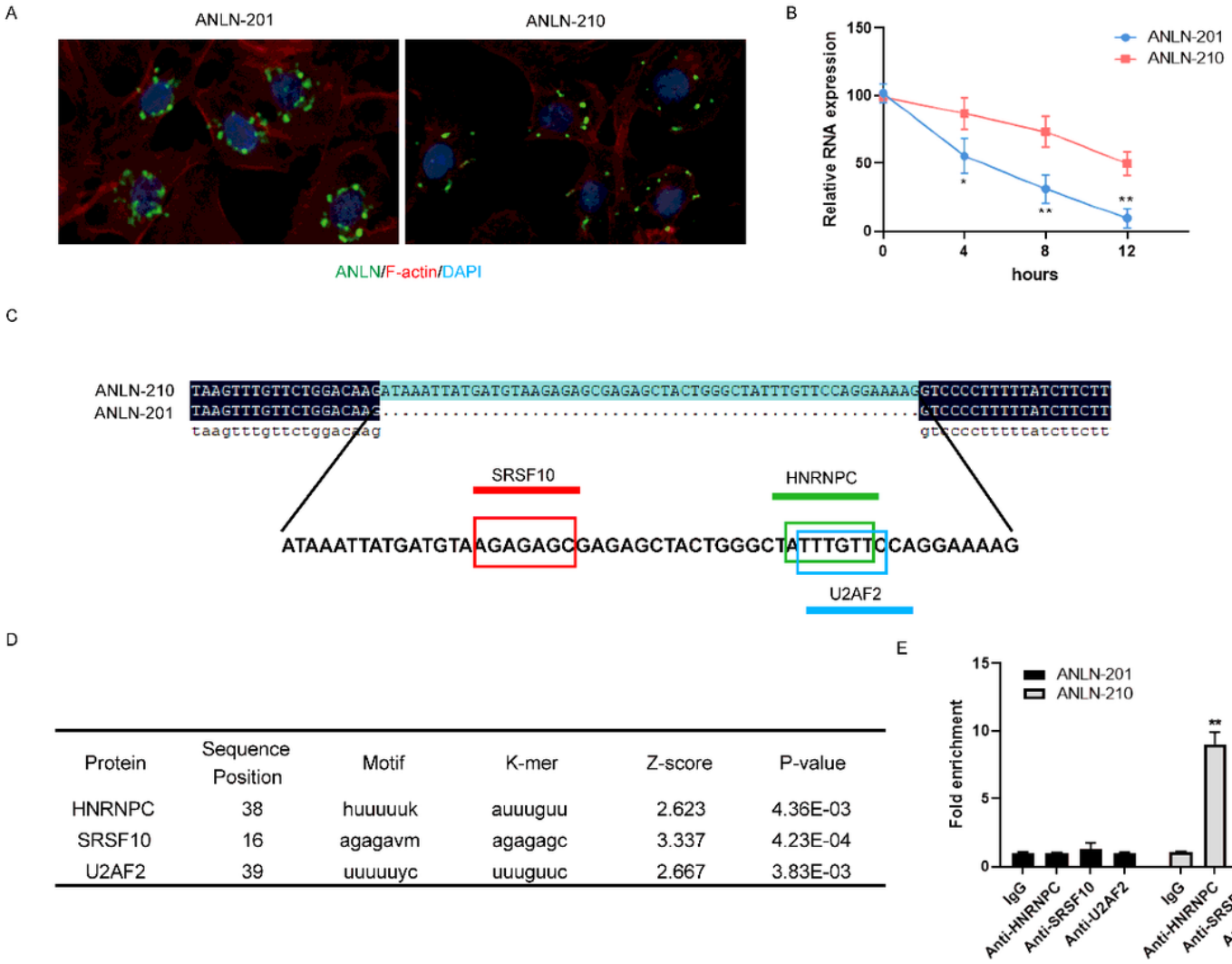

Protein	Sequence Position	Motif	K-mer	Z-score	P-value
HNRNPC	38	huuuuuk	auuuguu	2.623	4.36E-03
SRSF10	16	agagavm	agagagc	3.337	4.23E-04
U2AF2	39	uuuuuyc	uuuguuc	2.667	3.83E-03

Figure 4

The subcellular distribution and predicted RNA binding protein of ANLN RNA splicing in SCC-9 cells. (A) Immunofluorescence staining for ANLN-201 and ANLN-210 in SCC-9 cells. (B) The mRNA levels of ANLN-201 and ANLN-210 were examined at 4, 8, 12 hours after treated with actinomycin D. **p□0.05, * p□0.01. (C) Sequence alignment of nucleotides between ANLN-210 and ANLN-201. (D) The predicted RNA binding protein with ANLN-210 were listed in the table. (E) RNA co-immunoprecipitation was performed between ANLN-201/ANLN-210 and HNRNPC/SRSF10/U2AF2. *p□0.05, ** p□0.01.

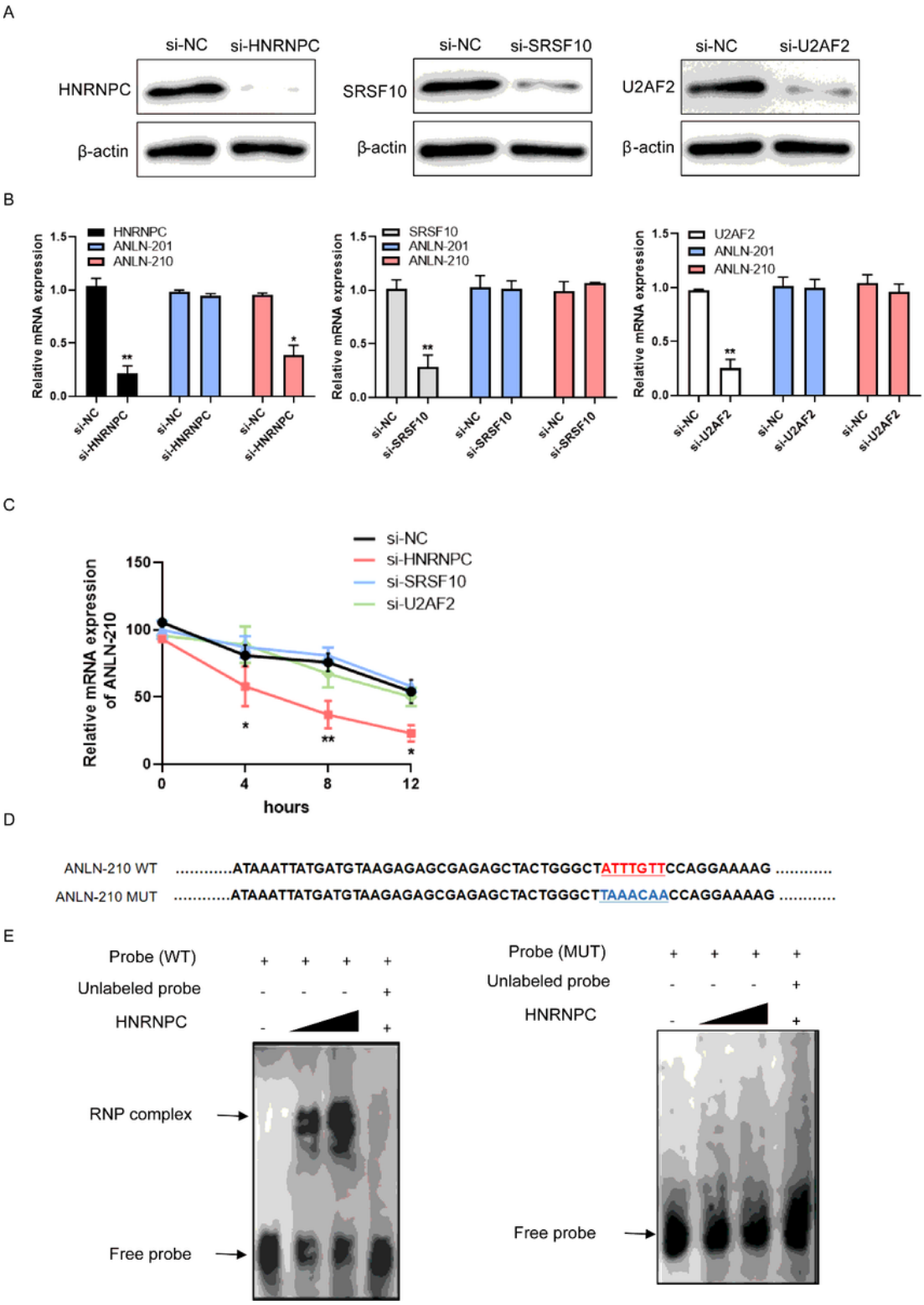

Figure 5

ANLN-210 mRNA interacts with HNRNPC. (A) The knockdown efficiency of si-HNRNPC, si-SRSF10 and si-U2AF2 was assessed at protein level by western blot. (B) The RNA levels of ANLN-201 or ANLN-210 were measured by qRT-PCR. *p□0.05, ** p□0.01. (C) The RNA stability of ANLN-210 was evaluated in si-HNRNPC or si-SRSF10 or si-U2AF2 treated with actinomycin D after 4, 8, 12 hours. (D) The wildtype and mutant

binding sites between ANLN-210 and HNRNPC. (E) The interaction between ANLN-210 and HNRNPC was performed by the in vitro gel block experiment.

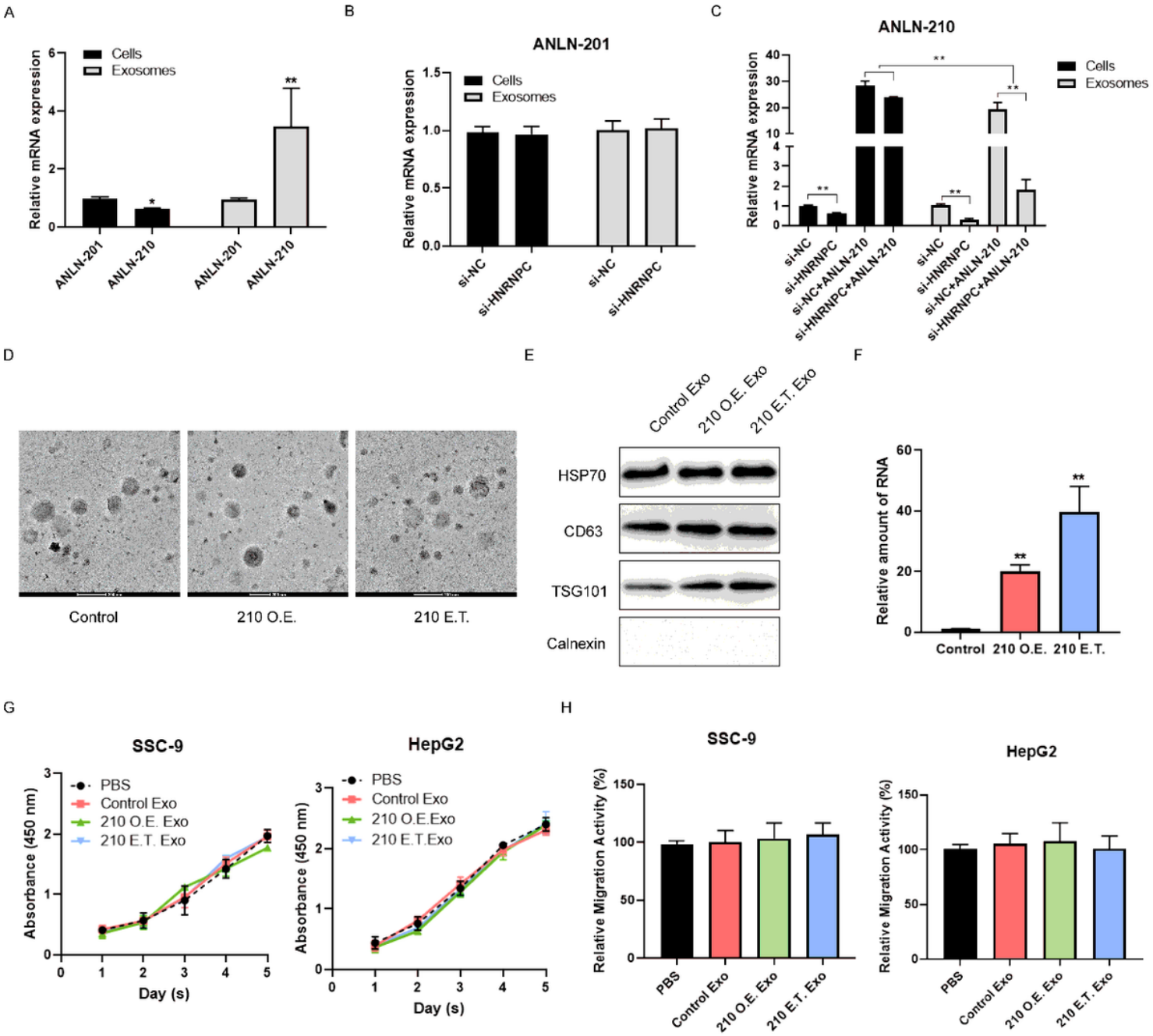

Figure 6

Expression pattern and functional effects of two ANLN RNA splicing in exosomes. (A) The expression of ANLN-201 and ANLN-210 was examined in cells and exosomes by qRT-PCR. * p□0.05, **p□0.01. (B) The expression of ANLN-201 at mRNA level was examined in SCC-9 cells and exosomes when SCC-9 cells were transfected with si-HNRNPC. (C) The expression of ANLN-210 at mRNA level was examined in SCC-9 cells and exosomes when cells were transfected with si-HNRNPC and ANLN-210 overexpression. * p□0.05, **p□0.01. (D) The representative images of exosomes were extracted from SCC-9 cells transfected with ANLN-210 overexpression or exosomes were electrotransfected with ANLN-210. (E) Exosomal markers

HSP70, CD63, TSG101 in isolated exosomes and calnexin expression in cell lysates as the control were examined by western blot. (F) The relative expression of ANLN-210 was examined in exosomes derived from SCC-9 cells transfected with ANLN-210 overexpression, exosomes electrotransfected with ANLN-210 and exosomes derived from control SCC-9 cells with ANLN-knockout. (G) Cell proliferation was performed in SCC-9 cell or HepG2 cells with the following treatment. PBS, exosomes derived from cells with ANLN knockout, exosomes derived from cells ANLN overexpression and exosomes electrotransfected with ANLN-210. (H) Cell migration and invasion were analyzed in SCC-9 cells treated with the following treatment. PBS, exosomes derived from cells with ANLN knockout, exosomes derived from cells ANLN overexpression and exosomes electrotransfected with ANLN-210.

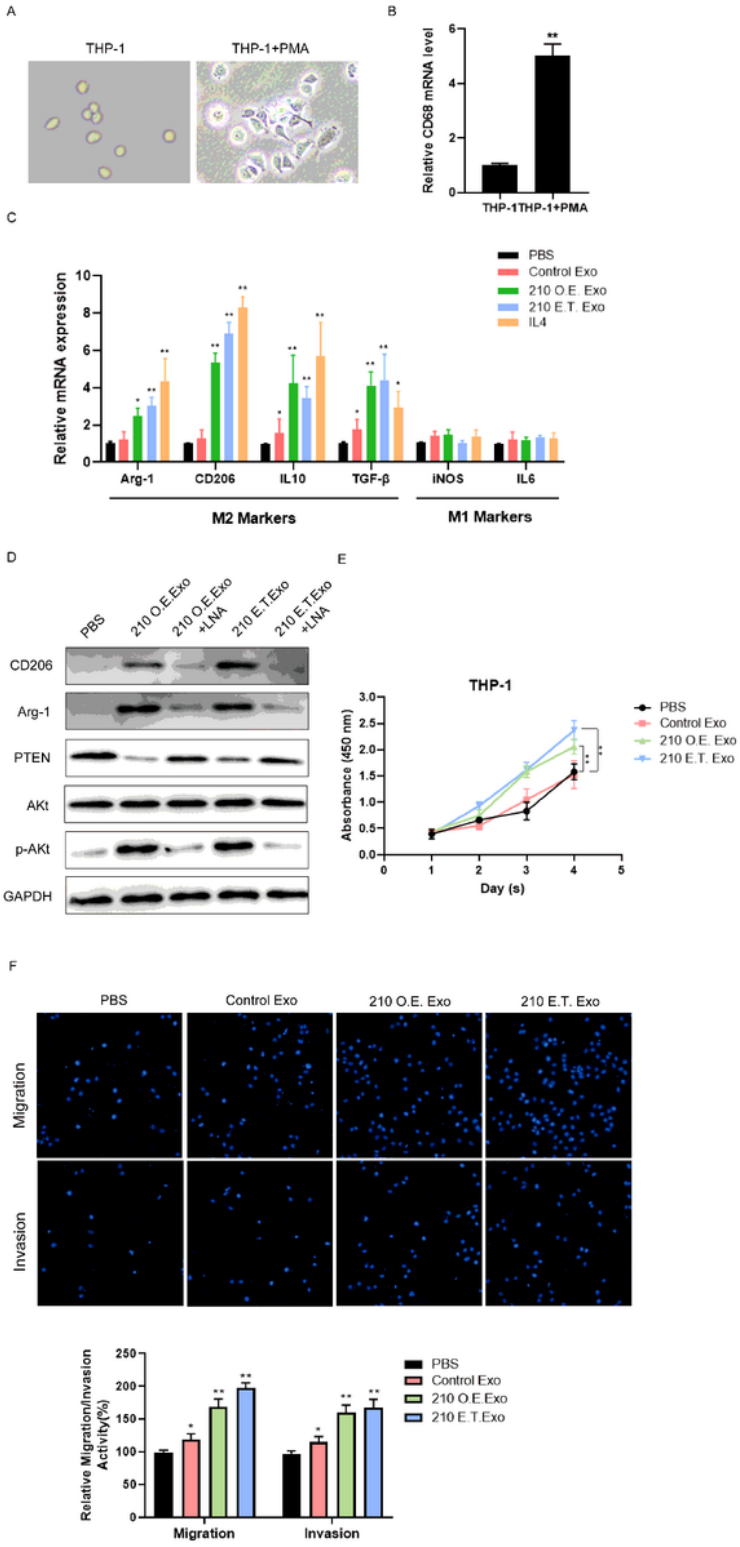

Figure 7

Expression pattern and functional effects of two ANLN RNA splicing in exosomes. (A) The expression of ANLN-201 and ANLN-210 was examined in cells and exosomes by qRT-PCR. * p□0.05, **p□0.01. (B) The expression of ANLN-201 at mRNA level was examined in SCC-9 cells and exosomes when SCC-9 cells were transfected with si-HNRNPC. (C) The expression of ANLN-210 at mRNA level was examined in SCC-9 cells and exosomes when cells were transfected with si-HNRNPC and ANLN-210 overexpression. * p□0.05,

**p□0.01. (D) The representative images of exosomes were extracted from SCC-9 cells transfected with ANLN-210 overexpression or exosomes were electrotransfected with ANLN-210. (E) Exosomal markers HSP70, CD63, TSG101 in isolated exosomes and calnexin expression in cell lysates as the control were examined by western blot. (F) The relative expression of ANLN-210 was examined in exosomes derived from SCC-9 cells transfected with ANLN-210 overexpression, exosomes electrotransfected with ANLN-210 and exosomes derived from control SCC-9 cells with ANLN-knockout. (G) Cell proliferation was performed in SCC-9 cell or HepG2 cells with the following treatment. PBS, exosomes derived from cells with ANLN knockout, exosomes derived from cells ANLN overexpression and exosomes electrotransfected with ANLN-210. (H) Cell migration and invasion were analyzed in SCC-9 cells treated with the following treatment. PBS, exosomes derived from cells with ANLN knockout, exosomes derived from cells ANLN overexpression and exosomes electrotransfected with ANLN-210.

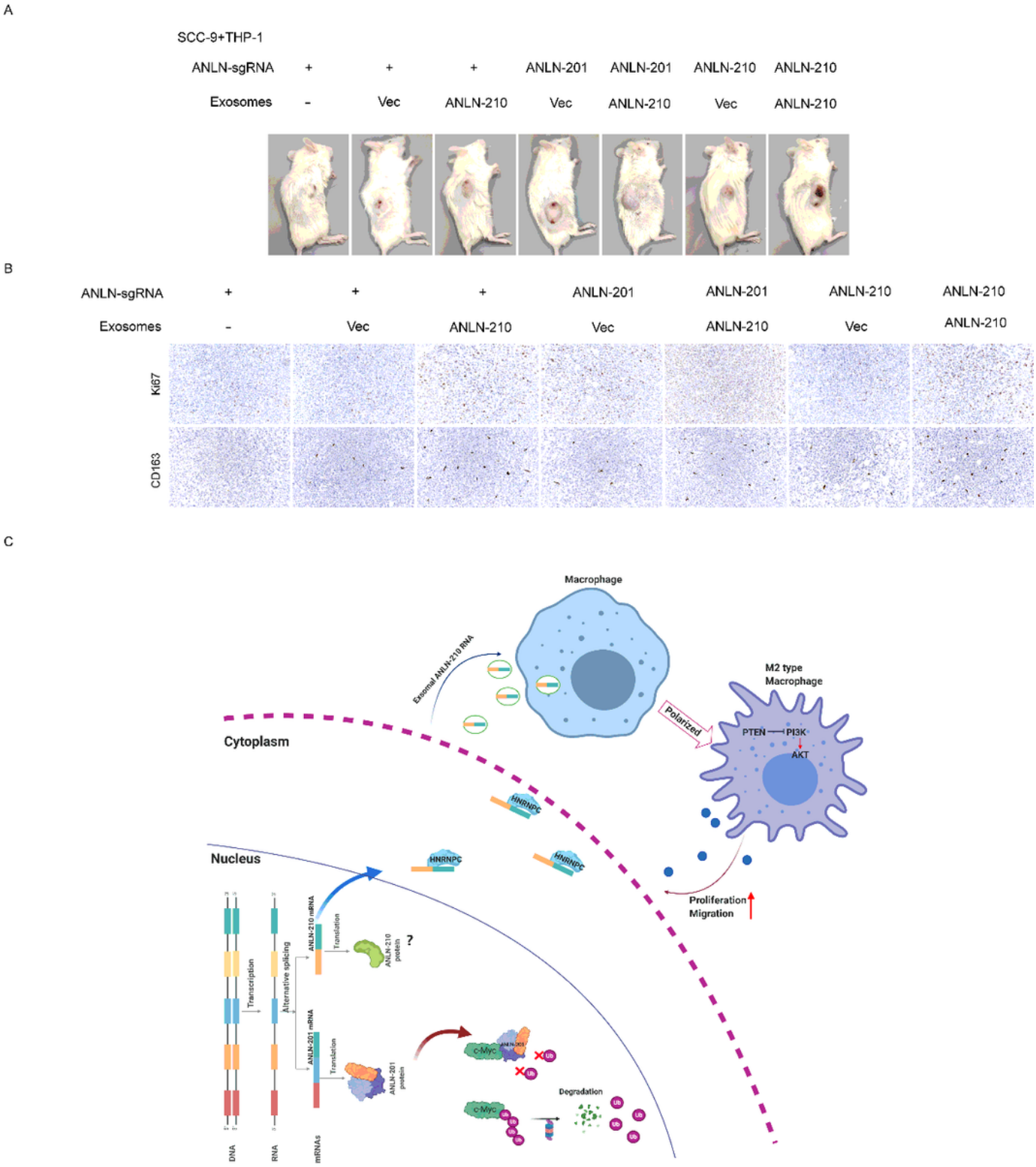

Figure 8

Two ANLN alternative splicing synergistically promote HNSCC tumor growth. (A) Representative images of HNSCC tumors from mice co-injected with SCC-9 cells plus THP-1 cells treated with exosomes (4:1) via the tail veins (n = 3). The experiment groups were as follows. ANLN-sgRNA SCC-9 cells and THP-1 treated with PBS, ANLN-sgRNA SCC-9 cells and THP-1 treated with exosomes secreted from control SCC-9 cells, ANLN-sgRNA SCC-9 cells and THP-1 treated with exosomes secreted from ANLN-210

overexpressed SCC-9 cells, ANLN-201-overexpressing SCC-9 cells and THP-1 cells treated with exosomes secreted from control SCC-9 cells, ANLN-201-overexpressing SCC-9 cells and THP-1 cells treated with exosomes secreted from ANLN-210-overexpresing SCC-9 cells, ANLN-210-overexpressing SCC-9 cells and THP-1 cells treated with exosomes secreted from control SCC-9 cells, ANLN-210-overexpressing SCC-9 cells and THP-1 cells treated with exosomes secreted from ANLN-210-overexpresing SCC-9 cells. (B) Representative immunohistochemistry analysis of the expression of CD163 and Ki67 in the xenograft tumor tissues. The groups were listed as above. (C) Schematic illustration of the regulatory mechanism of ANLN RNA splicing in the promotion of HNSCC progression.

Supplementary Files

This is a list of supplementary files associated with this preprint. Click to download.

- FigS1.png